Analysis of Laminated Composites and Sandwich Structures by Trigonometric, Exponential and Miscellaneous Polynomials and a MITC9 Plate Element

M. Filippi[1], M. Petrolo[1], S. Valvano[1], E. Carrera[1]

(1) Department of Mechanical and Aerospace Engineering,
Politecnico di Torino, Turin, Italy

Keywords:
Trigonometric, Exponential, Finite Element Method, Mixed Interpolation of Tensorial Components, Carrera Unified Formulation, Plate.

Author and address for Correspondence
Dr. Matteo Filippi
Research Assistant,
Department of Mechanical and Aerospace Engineering
Politecnico di Torino,
Corso Duca degli Abruzzi, 24,
10129 Torino, ITALY,
tel +39.011.090.6887, fax +39.011.090.6899
e.mail: matteo.filippi@polito.it

Abstract

This paper proposes some advanced plate theories obtained by expanding the unknown displacement variables along the thickness direction using trigonometric series, exponential functions and miscellaneous polynomials. The used refined models are Equivalent Single Layer (ESL) theories. They are obtained by means of the Unified Formulation by Carrera (CUF), and they accurately describe the displacement field and the stress distributions along the thickness of the multilayered plate. The governing equations are derived from the Principle of Virtual Displacement (PVD), and the Finite Element Method (FEM) is employed to solve them. The plate element has nine nodes, and the Mixed Interpolation of Tensorial Components (MITC) method is used to contrast the membrane and shear locking phenomenon. Cross-ply plates with simply-supported edges and subjected to a bi-sinusoidal load, and sandwich plates with simply-supported edges and subjected to a constant transverse uniform pressure are analyzed. Various thickness ratios are considered. The results, obtained with different theories within CUF, are compared with the elasticity solutions given in the literature and the layer-wise solution. It is shown that refined kinematic theories employing trigonometric or exponential terms are able to accurately describe the displacment field and the mechanical stress fields. In some cases, the reduction of computational costs is particularly relevant respect to the layer-wise solution.

1 Introduction

Composite plate/shell structures have a predominant role in many engineering applications. Structural models for composite plates must be able to deal with a number of physical effects such as anisotropy, shear deformation and interlaminar continuity of shear stress. Analytical, closed form solutions are available in very few cases. In most of the practical problems, the solution demands applications of approximated computational methods. The Finite Element Method (FEM) has a predominant role among the computational techniques implemented for the analysis of layered structures. Finite elements are usually formulated on the basis of axiomatic-type theories, in which the unknown variables are postulated along the thickness. According to published research, various theories for composite structures have been developed. They can be classified as: Equivalent Single Layer (ESL), in which the number of unknowns is independent of the number of layers, and Layer-wise approach (LW), in which the number of unknowns is dependent on the number of layers. The simplest plate/shell theory is based on the Kirchoff/Love's hypothesis, and it is usually referred to as Classical Lamination Theory (CLT)[1, 2]. The inclusion of transverse shear strains leads to the Reissner-Mindlin Theory, also known

as First-order Shear Deformation Theory (FSDT) [3]. A review of equivalent single layer and layer-wise laminate theories was presented by Reddy [4]. Also, a large variety of plate/shell finite element implementations of higher-order theories (HOT) has been proposed in the last twenty years. HOT-type theories were discussed by Kant and co-authors [5, 6], by Reddy [7] and Palazotto and Dennis [8].
Concerning trigonometric polynomial expansions, some plate and beam theories have been developed. Shimpi and Ghugal [9] used trigonometric terms in the displacements field for the analysis of two layers composite beams. An ESL model was developed by Arya et al. [10] using a sine term to represent the non-linear displacement field across the thickness in symmetrically laminated beams. An extension of [10] to composite plates was presented by Ferreira et al. [11]. A trigonometric shear deformation theory is used to model symmetric composite plates discretized by a meshless method based on global multiquadric radial basis functions. A version of this theory, with a layer-wise approach, was proposed by the same authors in [12]. Vidal and Polit [13] developed a new three-noded beam finite element for the analysis of laminated beams, based on a sine distribution with layer refinement. Recently, the same authors have dealt with the influence of the Murakami's zig-zag function in the sine model for static and vibration analysis of laminated beams [14]. Static and free vibration analysis of laminated shells were performed by radial basis functions collocation, according to a sinusoidal shear deformation theory in Ferreira et al. [15]. It accounts for through-the-thickness deformation, by considering a sinusoidal evolution of all displacements along the thickness coordinate. The complexity of some structures often require to adopt a 3D model to correctly describe the mechanical behaviour, this is the most used solution of the commercial codes. Usually the computational costs of a 3D element are very relevant compared to a 1D or 2D element. A recent work recommends over-integration in conjunction with a 3D element [16].
In this work, an improved plate finite element is presented for the analysis of plate multilayered structures. It is based on the Carrera Unified Formulation (CUF), which was developed by Carrera for multi-layered structures [17, 18]. Within the CUF framework, several beam models using trigonometric, exponential, hyperbolic and miscellaneous series were employed [19, 20]. A review of equivalent single layer and layer-wise laminate theories was presented in [21]. In the present work, a number of advanced ESL plate theories, obtained by use of Taylor polynomials, trigonometric series, and exponential functions, are discussed. The Mixed Interpolation of Tensorial Components (MITC) method [22, 23, 24] is used to contrast the membrane and shear locking. The governing equations in weak form for the linear static analysis of composite structures are derived from the Principle of Virtual Displacement (PVD), and the finite element method is used to solve them. Cross-ply plates with simply-supported edges and subjected to a bi-sinusoidal load, and sandwich plates with simply-supported edges and sub-

jected to a constant transverse uniform pressure are analyzed. The results, obtained with the different models, are compared with both exact solutions and higher-order theories solutions given in literature. This paper is organized as follows: geometrical and constitutive relations for plates are presented in Section 2. In Section 3, an overview of classical, higher-order and advanced plate theories developed within the CUF framework is given. Section 4 gives a brief outline of the FEM approach and the MITC9 method to overcome the problem of shear locking, whereas, in Section 5, the governing equations in weak form for the linear static analysis of composite structures are derived from the PVD. In Section 6, the results obtained using the proposed CUF theories are discussed. Section 7 is devoted to the conclusions.

2 Geometrical and constitutive relations for plates

Plates are bi-dimensional structures in which one dimension (in general the thickness in the z direction) is negligible with respect to the other two in-plane dimensions. The geometry and the reference system are indicated in Figure 1. Geometrical relations enable to express the in-plane $\boldsymbol{\epsilon}_p^k$ and out-plane $\boldsymbol{\epsilon}_n^k$ strains in terms of the displacement $\boldsymbol{u}$:

$$\boldsymbol{\epsilon}_p^k = [\epsilon_{xx}^k, \epsilon_{yy}^k, \epsilon_{xy}^k]^T = (\boldsymbol{D}_p^k)\ \boldsymbol{u}^k\ ,\ \boldsymbol{\epsilon}_n^k = [\epsilon_{xz}^k, \epsilon_{yz}^k, \epsilon_{zz}^k]^T = (\boldsymbol{D}_{np}^k + \boldsymbol{D}_{nz}^k)\ \boldsymbol{u}^k\ . \tag{1}$$

The explicit form of the introduced arrays of the differential operators is:

$$\boldsymbol{D}_p^k = \begin{bmatrix} \partial_x & 0 & 0 \\ 0 & \partial_y & 0 \\ \partial_y & \partial_x & 0 \end{bmatrix}, \quad \boldsymbol{D}_{np}^k = \begin{bmatrix} 0 & 0 & \partial_x \\ 0 & 0 & \partial_y \\ 0 & 0 & 0 \end{bmatrix}, \quad \boldsymbol{D}_{nz}^k = \begin{bmatrix} \partial_z & 0 & 0 \\ 0 & \partial_z & 0 \\ 0 & 0 & \partial_z \end{bmatrix}, \tag{2}$$

The stress-strain relations are:

$$\begin{aligned} \boldsymbol{\sigma}_p^k &= \boldsymbol{C}_{pp}^k\ \boldsymbol{\epsilon}_p^k + \boldsymbol{C}_{pn}^k\ \boldsymbol{\epsilon}_n^k \\ \boldsymbol{\sigma}_n^k &= \boldsymbol{C}_{np}^k\ \boldsymbol{\epsilon}_p^k + \boldsymbol{C}_{nn}^k\ \boldsymbol{\epsilon}_n^k \end{aligned} \tag{3}$$

where

$$\begin{aligned} \boldsymbol{C}_{pp}^k &= \begin{bmatrix} C_{11}^k & C_{12}^k & C_{16}^k \\ C_{12}^k & C_{22}^k & C_{26}^k \\ C_{16}^k & C_{26}^k & C_{66}^k \end{bmatrix} \qquad \boldsymbol{C}_{pn}^k = \begin{bmatrix} 0 & 0 & C_{13}^k \\ 0 & 0 & C_{23}^k \\ 0 & 0 & C_{36}^k \end{bmatrix} \\ \boldsymbol{C}_{np}^k &= \begin{bmatrix} 0 & 0 & 0 \\ 0 & 0 & 0 \\ C_{13}^k & C_{23}^k & C_{36}^k \end{bmatrix} \qquad \boldsymbol{C}_{nn}^k = \begin{bmatrix} C_{55}^k & C_{45}^k & 0 \\ C_{45}^k & C_{44}^k & 0 \\ 0 & 0 & C_{33}^k \end{bmatrix} \end{aligned} \tag{4}$$

For the sake of brevity, the expressions, that relate the material coefficients C_{ij} to the Young's moduli E_1, E_2, E_3, the shear moduli G_{12}, G_{13}, G_{23} and Poisson moduli ν_{12}, ν_{13}, ν_{23}, ν_{21}, ν_{31}, ν_{32} that characterize the layer material, are not given here. They can be found in [4].

3 Carrera Unified Formulation for Plates

According to the CUF [18, 25, 26], the displacement field can be written as follows:

$$\begin{cases} u(x,y,z) = F_0(x,y)\, u_0(x,y) + F_1\, u_1(x,y) + ... + F_N\, u_N(x,y) \\ v(x,y,z) = F_0(x,y)\, v_0(x,y) + F_1\, v_1(x,y) + ... + F_N\, v_N(x,y) \\ w(x,y,z) = F_0(x,y)\, w_0(x,y) + F_1\, w_1(x,y) + ... + F_N\, w_N(x,y) \end{cases} \tag{5}$$

In compact form:

$$\boldsymbol{u}^k(x,y,z) = F_s(z)\boldsymbol{u}_s^k(x,y); \qquad \delta\boldsymbol{u}^k(x,y,z) = F_\tau(z)\delta\boldsymbol{u}_\tau^k(x,y) \qquad \tau, s = 0, 1, ..., N \tag{6}$$

where (x, y, z) is the general reference system, see Figure 1, and the displacement vector $\boldsymbol{u} = \{u, v, w\}$ has its components expressed in this system. $\delta\boldsymbol{u}$ is the virtual displacement associated to the virtual work and k identifies the layer. F_τ and F_s are the thickness functions depending only on z. $\boldsymbol{u}_s$ are the unknown variables depending on the coordinates x and y. τ and s are sum indexes and N is the number of terms of the expansion in the thickness direction assumed for the displacements.

3.1 Taylor Higher-order Theories

Many attempts have been made to improve classical plate models. The CUF has the capability to expand each displacement variable at any desired order. Each variable can be treated independently from the others ones according to the requested accuracy. This procedure becomes extremely useful when multifield problems are investigated such as thermoelastic and piezoelectric applications [27, 28, 29].

In the case of ESL models, a Taylor expansion is employed as thickness functions:

$$\boldsymbol{u} = F_0\, \boldsymbol{u}_0 + F_1\, \boldsymbol{u}_1 + \ldots + F_N\, \boldsymbol{u}_N = F_s\, \boldsymbol{u}_s, \qquad s = 0, 1, \ldots, N. \tag{7}$$

$$F_0 = z^0 = 1, \quad F_1 = z^1 = z, \quad \ldots, \quad F_N = z^N. \tag{8}$$

For Taylor polynomials, the letter N indicates the number of terms of the expansion and the polynomial order. Following this approach the displacement field can be written as:

$$\begin{cases} u(x,y,z) = u_0(x,y) + z\,u_1(x,y) + ... + z^N\,u_N(x,y) \\ v(x,y,z) = v_0(x,y) + z\,v_1(x,y) + ... + z^N\,v_N(x,y) \\ w(x,y,z) = w_0(x,y) + z\,w_1(x,y) + ... + z^N\,w_N(x,y) \end{cases} \tag{9}$$

For example, the theory $ET2$ refers to the following displacement field:

$$\boldsymbol{u}^k(x,y,z) = \boldsymbol{u}_0^k(x,y) + z\,\boldsymbol{u}_1^k(x,y) + z^2\,\boldsymbol{u}_2^k(x,y) \tag{10}$$

Classical models, such as the First-order Shear Deformation Theory (FSDT), can be obtained from an ESL theory with $N = 1$, by imposing a constant transverse displacement through the thickness via penalty techniques. Also, a model based on the hypotheses of CLT can be expressed using the CUF by applying a penalty technique to the constitutive equations.

3.2 Advanced Trigonometric and Exponential expansion Theories

If a trigonometric sine series plus a constant contribution is adopted, the displacement variables can be written as follows:

$$\boldsymbol{u}^k(x,y,z) = \boldsymbol{u}_0^k(x,y) + sin\left(\frac{\pi z}{h}\right)\,\boldsymbol{u}_1^k(x,y) + ... + sin\left(\frac{n\pi z}{h}\right)\,\boldsymbol{u}_N^k(x,y) \tag{11}$$

where h is the whole thickness dimension and n is the half-waves number. If the linear contribution is considered, the displacement expression is:

$$\boldsymbol{u}^k(x,y,z) = \boldsymbol{u}_0^k(x,y) + z\,\boldsymbol{u}_1^k(x,y) + sin\left(\frac{\pi z}{h}\right)\,\boldsymbol{u}_2^k(x,y) + ... + sin\left(\frac{n\pi z}{h}\right)\,\boldsymbol{u}_{N+1}^k(x,y) \tag{12}$$

A similar description can be provided using a trigonometric cosine series:

$$\boldsymbol{u}^k(x,y,z) = \boldsymbol{u}_0^k(x,y) + cos\left(\frac{\pi z}{h}\right)\,\boldsymbol{u}_1^k(x,y) + ... + cos\left(\frac{n\pi z}{h}\right)\,\boldsymbol{u}_N^k(x,y) \tag{13}$$

and with the linear contribution:

$$\boldsymbol{u}^k(x,y,z) = \boldsymbol{u}_0^k(x,y) + z\,\boldsymbol{u}_1^k(x,y) + cos\left(\frac{\pi z}{h}\right)\,\boldsymbol{u}_2^k(x,y) + ... + cos\left(\frac{n\pi z}{h}\right)\,\boldsymbol{u}_{N+1}^k(x,y) \tag{14}$$

A complete trigonometric series becomes:

$$\begin{aligned} \boldsymbol{u}^k(x,y,z) = \boldsymbol{u}_0^k(x,y) + sin\left(\frac{\pi z}{h}\right)\,\boldsymbol{u}_1^k(x,y) + cos\left(\frac{\pi z}{h}\right)\,\boldsymbol{u}_2^k(x,y) + ... + sin\left(\frac{n\pi z}{h}\right)\,\boldsymbol{u}_{2N-1}^k(x,y) + \\ + cos\left(\frac{n\pi z}{h}\right)\,\boldsymbol{u}_{2N}^k(x,y) \end{aligned} \tag{15}$$

If the linear contribution is considered:

$$\begin{aligned}\boldsymbol{u}^k(x,y,z) = \boldsymbol{u}_0^k(x,y) + z\,\boldsymbol{u}_1^k(x,y) + sin\left(\frac{\pi z}{h}\right)\,\boldsymbol{u}_2^k(x,y) + cos\left(\frac{\pi z}{h}\right)\,\boldsymbol{u}_3^k(x,y) + ...+ \\ + sin\left(\frac{n\pi z}{h}\right)\,\boldsymbol{u}_{2N}^k(x,y) + cos\left(\frac{n\pi z}{h}\right)\,\boldsymbol{u}_{2N+1}^k(x,y)\end{aligned} \tag{16}$$

If an exponential expansion is employed the displacement field is:

$$\boldsymbol{u}^k(x,y,z) = \boldsymbol{u}_0^k(x,y) + e^{(z/h)}\,\boldsymbol{u}_1^k(x,y) + ... + e^{(nz/h)}\,\boldsymbol{u}_N^k(x,y) \tag{17}$$

and adding the linear contribution:

$$\boldsymbol{u}^k(x,y,z) = \boldsymbol{u}_0^k(x,y) + z\,\boldsymbol{u}_1^k(x,y) + e^{(z/h)}\,\boldsymbol{u}_2^k(x,y) + ... + e^{(nz/h)}\,\boldsymbol{u}_{N+1}^k(x,y) \tag{18}$$

3.3 Refined theories with Zig-Zag Models

Due to the intrinsic anisotropy of multilayered structures, the first derivative of the displacement variables in the z-direction is discontinuous. It is possible to reproduce the zig-zag effects in the framework of the ESL description by employing the Murakami theory. According to [30], a zig-zag term can be introduced into equation(7) as follows:

$$\boldsymbol{u}^k = \; F_0\,\boldsymbol{u}_0^k \; + \; \ldots \; + \; F_N\,\boldsymbol{u}_N^k \; + \; (-1)^k\zeta_k\boldsymbol{u}_Z^k. \tag{19}$$

Subscript Z refers to the introduced term. Such theories are called zig-zag theories. Following this approach the displacement field can be written as:

$$\begin{cases} u(x,y,z) = F_0(x,y)\,u_0(x,y) + F_1\,u_1(x,y) + ... + F_{N-1}\,u_{N-1}(x,y) + (-1)^k\zeta_k u_{N_Z}^k \\ v(x,y,z) = F_0(x,y)\,v_0(x,y) + F_1\,v_1(x,y) + ... + F_{N-1}\,v_{N-1}(x,y) + (-1)^k\zeta_k v_{N_Z}^k \\ w(x,y,z) = F_0(x,y)\,w_0(x,y) + F_1\,w_1(x,y) + ... + F_{N-1}\,w_{N-1}(x,y) + (-1)^k\zeta_k w_{N_Z}^k \end{cases} \tag{20}$$

These refined theories can be obtained adding the zig-zag term to the Taylor polynomials expansions or the trigonometric and exponential ones.

3.4 Acronyms

A system of acronyms is given to denote the considered kinematic models. The first letters indicate the used approach in this work that is Equivalent Single Layer E. Sometimes a reference solution is given with a layer-wise approach, the first letters become LW. The second letter indicates the kind of employed function, T for Taylor polynomials, S for sines expansions, C for cosines expansions. The

number N indicates the number of the expansion terms (except the constant term) used in the thickness direction. The last letter Z is added if the zig-zag term is considered. If the Navier analytical method is employed the subscript (a) is used. The considered expansion are summarized in Table 1. For example, the theory $ET1S2Z$ refers to the following displacement field:

$$\boldsymbol{u}^k(x,y,z) = \boldsymbol{u}_0^k(x,y) + z\,\boldsymbol{u}_1^k(x,y) + sin\left(\frac{1\pi z}{h}\right)\boldsymbol{u}_2^k(x,y) + sin\left(\frac{2\pi z}{h}\right)\boldsymbol{u}_3^k(x,y) + (-1)^k\zeta_k\boldsymbol{u}_{4_Z}^k \quad (21)$$

4 Finite Element approximation and MITC9 method

In this section, the derivation of a plate finite element for the analysis of multilayered structures is presented. Considering a 9-node finite element, the displacement components are interpolated on the nodes of the element by means of the Lagrangian shape functions N_i:

$$\boldsymbol{u}_s = N_j\boldsymbol{u}_{s_j} \qquad \delta\boldsymbol{u}_\tau = N_i\delta\boldsymbol{u}_{\tau_i} \qquad \text{with} \quad i,j = 1,...,9 \quad (22)$$

where $\boldsymbol{u}_{s_j}$ and $\delta\boldsymbol{u}_{\tau_i}$ are the nodal displacements and their virtual variations. Therefore, equation (1) becomes:

$$\begin{aligned}\boldsymbol{\epsilon}_p =& F_s(\boldsymbol{D}_p)(N_j\boldsymbol{I})\boldsymbol{u}_{s_j}\\ \boldsymbol{\epsilon}_n =& F_s(\boldsymbol{D}_{np})(N_j\boldsymbol{I})\boldsymbol{u}_{s_j} + F_{s_{,z}}(N_j\boldsymbol{I})\boldsymbol{u}_{s_j}\end{aligned} \quad (23)$$

where $\boldsymbol{I}$ is the identity matrix. Considering the local coordinate system (ξ,η), the MITC plate elements ([31]-[32]) are formulated by using, instead of the strain components directly computed from the displacements, an interpolation of these within each element using a specific interpolation strategy for each component. The corresponding interpolation points, called *tying points*, are shown in Figure 2 for a nine-node element. Note that the normal transverse strain ϵ_{zz} is excluded from this procedure, and it is directly calculated from the displacements.

The interpolating functions are Lagrangian functions and are arranged in the following arrays:

$$\begin{aligned}N_{m1} &= [N_{A1}, N_{B1}, N_{C1}, N_{D1}, N_{E1}, N_{F1}]\\ N_{m2} &= [N_{A2}, N_{B2}, N_{C2}, N_{D2}, N_{E2}, N_{F2}]\\ N_{m3} &= [N_P, N_Q, N_R, N_S]\end{aligned} \quad (24)$$

Hereafter the subscripts $m1$, $m2$ and $m3$ indicate quantities calculated in the points $(A1, B1, C1, D1, E1, F1)$, $(A2, B2, C2, D2, E2, F2)$ and (P, Q, R, S), respectively. Therefore, the strain components are interpolated as follows:

$$\begin{aligned}
\boldsymbol{\epsilon}_p &= \begin{bmatrix} \epsilon_{xx} \\ \epsilon_{yy} \\ \epsilon_{xy} \end{bmatrix} = \begin{bmatrix} N_{m1} & 0 & 0 \\ 0 & N_{m2} & 0 \\ 0 & 0 & N_{m3} \end{bmatrix} \begin{bmatrix} \epsilon_{xx_{m1}} \\ \epsilon_{yy_{m2}} \\ \epsilon_{xy_{m3}} \end{bmatrix} \\
\boldsymbol{\epsilon}_n &= \begin{bmatrix} \epsilon_{xz} \\ \epsilon_{yz} \\ \epsilon_{zz} \end{bmatrix} = \begin{bmatrix} N_{m1} & 0 & 0 \\ 0 & N_{m2} & 0 \\ 0 & 0 & 1 \end{bmatrix} \begin{bmatrix} \epsilon_{xz_{m1}} \\ \epsilon_{yz_{m2}} \\ \epsilon_{zz} \end{bmatrix}
\end{aligned} \tag{25}$$

where the strains $\epsilon_{xx_{m1}}$, $\epsilon_{yy_{m2}}$, $\epsilon_{xy_{m3}}$, $\epsilon_{xz_{m1}}$, $\epsilon_{yz_{m2}}$ are expressed through equation (23) where the shape functions N_i and their derivatives are evaluated in the tying points.

5 Governing FEM equations

The PVD for a multilayered plate structure reads:

$$\int_{\Omega_k} \int_{A_k} \left\{ \delta \boldsymbol{\epsilon}_p^{k\,T} \boldsymbol{\sigma}_p^k + \delta \boldsymbol{\epsilon}_n^{k\,T} \boldsymbol{\sigma}_n^k \right\} \, d\Omega_k dz = \delta L_e \tag{26}$$

where Ω_k and A_k are the integration domains in the plane and the thickness direction, respectively. The left-hand side of the equation represents the variation of the internal work, while the right-hand side is the virtual variation of the external work.

Substituting the constitutive equations (3), the geometrical relations written via the MITC method (25) and applying the CUF (6) and the FEM approximation (22), one obtains the following governing equations:

$$\delta \boldsymbol{q}^{k\tau i} : \quad \boldsymbol{K}^{k\tau sij} \boldsymbol{q}^{ksj} = \quad \boldsymbol{P}^{k\tau i} \tag{27}$$

where $\boldsymbol{K}^{k\tau sij}$ is a 3×3 matrix, called fundamental nucleus of the mechanical stiffness matrix, and its explicit expression is given in [33]. The nucleus is the basic element from which the stiffness matrix of the whole structure is computed. The fundamental nucleus is expanded on the indexes τ and s to obtain the stiffness matrix of each layer k. Then, the matrixes of each layer are assembled at the multi-layer level depending on the approach considered, for this work the ESL approach is adopted.

$\boldsymbol{P}^{k\tau i}$ is a 3×1 matrix, called fundamental nucleus of the external load. $\boldsymbol{q}^{ksj}$ and $\delta\boldsymbol{q}^{k\tau i}$ are the nodal displacements and its variation respectively.

6 Numerical results

To assess the trigonometric and the exponential polynomial expansions the following reference problems have been considered in this section:

- A three-layer cross-ply square plate with lamination $(0°/90°/0°)$
- A two-layer cross-ply square plate with lamination $(0°/90°)$
- A four-layer cross-ply square plate with lamination $(0°/90°/90°/0°)$
- A three-layer rectangular sandwich plate

6.1 Three-layer cross-ply square plate $(0°/90°/0°)$

A three layered cross-ply square plate with lamination $(0°/90°/0°)$ and simply-supported boundary condition is considered. The applied load is:

$$p\left(x, y, z_{top}\right) = \hat{p}\, sin\left(\frac{m\pi x}{a}\right) sin\left(\frac{n\pi y}{b}\right) \tag{28}$$

where $m = n = 1$, see Figure 1. The mechanical properties of the material are: $E_L/E_T = 25$; $G_{LT}/E_T = 0,5$; $G_{TT}/E_T = 0,2$; $\nu_{LT} = \nu_{TT} = 0,25$. The geometrical dimensions are: $a = b = 1.0$. The mechanical load amplitude at the top position is: $\hat{p} = 1.0$. The results are presented for different thickness ratios $a/h = 4, 10, 100$, and reported in non-dimensional form:

$$\hat{w} = \frac{100 w E_T h^3}{\hat{p}\; a^4} \qquad ; \qquad \hat{\sigma}_{xx} = \frac{\sigma_{xx}}{\hat{p}\left(\frac{a}{h}\right)^2} \qquad ; \qquad \hat{\sigma}_{xz/yz} = \frac{\sigma_{xz/yz}}{\hat{p}\left(\frac{a}{h}\right)} \tag{29}$$

6.1.1 Convergence and locking study

First of all, a convergence study on the plate element has been performed. A composite plate with thickness ratio $a/h = 100$, is evaluated. The Navier-type solution with a Taylor polynomials expansion of the 4^{th} order has been taken as reference solution. It can be noticed that, evaluating the transverse displacement w and transverse shear stress σ_{xz}, the convergence is not depending on the different kinds of employed polynomials, see Table 2. A mesh grid of 10×10 elements ensures the convergence. Then a locking study has been performed evaluating different types of integration methods [34] for the same

plate structure to prove that the element is locking free, see Table 3. The plate element with the MITC9 method leads to accurate results in terms of both transverse displacement and shear stress.

For thick and thin plates $a/h = 4\,, 100$ the results are presented in Table 4 for various expansions. The values of the transversal displacement w, in-plane stress σ_{xx} and transverse shear stresses σ_{xz} and σ_{yz} are compared with the exact $3D$ elasticity solution [35], the analytical solution calculated with a Taylor's polynomial expansion of the 4^{th} order ($ET4_a$), and the FEM solution obtained with a Layer-Wise approach using a Legendre expansion of the 4^{th} order ($LW4$).
For thin plates, $a/h = 100$, the following considerations are drawn:

- Regarding the transverse displacement w the exponential function ($EExp4$), the cosine expansion ($ET1C1$) and its combinations with series of sine functions ($ES4C4$) are more accurate than sine functions ($ES5$), see Figure 3. It can be noticed that the use of the linear term ($ET1Exp3$, $ET1S2C2$) determines a significant improvement of the results with a lower number of degrees of freedom (DOFs). The addition of the zig-zag term improves the accuracy even if for the sine function ($ES5Z$, $ET1S3Z$), and its combination with cosine ($ES4C4Z$) the improvement is lower, see Figure 4.

- The in-plane stress σ_{xx} is accurately described by all functions with or without the zig-zag term.

- For the transverse shear stress σ_{xz} the sine and the exponential functions, with the linear contribution, are close to the Taylor polynomial series of the 4^{th} order, but at interfaces the continuity is not fulfilled. To overcome this problem, it has been employed the zig-zag function, see Figure 5. As expected the zig-zag term improves the results, this is true excepting for the cosine function, the sine, and their combination.

- The transverse normal stress σ_{zz} is accurately described by the cosine function and its combination with the sine series, see Figure 6. It can be noticed that the sine series and its combination with the linear contribution lead to a completely wrong description of the transverse normal stress.

For thick plates, $a/h = 4$, the following considerations are drawn:

- Regarding the transverse displacement w, the increase of the performance of exponential series, and the sine function instead of cosine ones is more evident than the thin case. Furthermore using the zig-zag term the results are very close to the exact solution, except for the cosine ($ET1C2Z$), see Figure 7. Moreover, it can be observed that the sine series ($ES5Z$, $ET1S3Z$) predict a linear displacement profile, while the exponential expansion is the best approximation of the solution.

- The in-plane stress σ_{xx} is not accurately described by the cosine function ($ET1C1$), see Figure 8. It can be noticed that the Taylor results at the lower interface give a minor discontinuity. Only adding the zig-zag function the results strongly agree with the solution, see Figure 9.

- For the transverse shear stress σ_{xz} at interfaces the continuity is not fulfilled, see Figure 10. Also in this case only the addition of the zig-zag term is able to improve the results, see Figure 11. Exept for the cosine series, all the employed functions can lead to good results. The discontinuity is very reduced and it is smaller than ones obtained by using Taylor polynomials.

- The transverse normal stress σ_{zz}, unlike the previous case $a/h = 100$, can be described correctly by the sine series too, see Figure 12. Adding the zig-zag term the results are closer to the exact solution, expecially the exponential expansion and the sine and cosine combination lead to very accurate results, see Figure 13.

For the thickness ratio $a/h = 10$ the results are presented in Table 5. The values of the transversal displacement w, in-plane stress σ_{xx} and transverse shear stresses σ_{xz} and σ_{yz} are compared with the exact $3D$ elasticity solution and with different reference solutions taken in the literature. For moderately thin plate, the following considerations are drawn:

- Regarding the transverse displacement w, the exponential series, and in particular the sine functions are more efficient than the cosine series. Furthermore, using the zig-zag term, except the cosine ($ET1C2Z$) and the sine series ($ES5Z$, $ET1S3Z$), the results are closer to the exact solution.

- The in-plane stress σ_{xx} is not correctly described as for thin plate $a/h = 100$, moreover the cosine function ($ET1C1$) does not match the solution. Only adding the zig-zag function the results match the exact solution.

- For the transverse shear stress σ_{xz}, also in this case, the addition of the zig-zag term to functions series is able to improve the results and to reduce the discontinuity. Execpt for the cosine series, all the functions employed can lead to accurate results.

- The transverse normal stress σ_{zz} is not accurately described by sine functions, see Figure 14, but this problem is reduced compared to the thin plate $a/h = 100$.

6.2 Two-layer ($0°/90°$) and four-layer ($0°/90°/90°/0°$) cross-ply square plate

The plates are simply-supported and different thickness ratios are studied. The geometrical and material properties are the same of the previous three-layer plate. The plate structures are loaded by the same bi-sinusoidal load pressure applied at the top surface.

For the 2 layered plate the results are listed in Table 6. As expected, for thin plates, $a/h = 100$, all the functions lead to accurate results. Despite the transverse displacement w and the in-plane principal stress σ_{xx} match the exact solution, the shear stresses σ_{xz} and σ_{yz} are not correctly described. For thick plates $a/h = 4$, the $ET4$ expansion underestimates the transverse displacement and the in-plane stress compared to the reference solution given by a layer-wise approach. All the results obtained by the proposed trigonometric and exponential expansions are close to the layer-wise solution more than the Taylor polynomial one. Furthermore, adding the zig-zag term to the expansion series, all the FE results achieve significant accuracy, also in terms of shear stresses. For the 4 layered plate the results are listed in Table 7. The values of the transversal displacement w are compared with the exact $3D$ elasticity solution and with different reference solutions available in the literature. It is clear that for thin plate all the FE results are close to the exact solution, conversely for thick plates the results match the exact solution only by adding the zig-zag function. It can be noticed that the zig-zag function strongly improves the solution, especially for thick plates. The reduction of computational costs is particularly relevant in some cases compared to the layer-wise solution.

6.3 Three-layer rectangular sandwich plate

A 3 layered, unsymmetrically laminated, rectangular sandwich plate has been analyzed. The plate is loaded by a constant uniform pressure $P_z^{top} = -0.1\,MPa$ applied to the whole top surface. The geometrical dimensions are: $a = 100\,mm$, $b = 200\,mm$, $h = 12\,mm$. The faces have different thickness: $h_{top} = 0.1\,mm$, $h_{bottom} = 0.5\,mm$, and the core thickness is $h_{core} = 11.4\,mm$. The two faces have the following material data: $E_1 = 70000\,MPa$, $E_2 = 71000\,MPa$, $E_3 = 69000\,MPa$, $G_{12} = G_{13} = G_{23} = 26000\,MPa$, $\nu_{12} = \nu_{13} = \nu_{23} = 0.3$. The core made of metallic foam has the following data: $E_1 = E_2 = 3\,MPa$, $E_3 = 2.8\,MPa$, $G_{12} = G_{13} = G_{23} = 1\,MPa$, $\nu_{12} = \nu_{13} = \nu_{23} = 0.25$.

The results of local values at top and bottom surfaces are listed in Table 8. It can be observed that although moderately thick plates are considered $a/h = (100/12)$, lower order theories as $ET1_a$ lead to completely wrong results. Very accurate models are required to capture the stress distribution in the two faces, and the importance of the zig-zag term has to be underlined for this type of layered

structure.

7 Conclusions

This paper has dealt with the static analysis of composite and sandwich plates by means of a two-dimensional finite element based on the Unified Formulation. The element has been assessed by analyzing cross-ply plates under bi-sinusoidal loads and simply-supported boundary conditions, and sandwich plates under a constant transverse uniform pressure. The results have been presented in terms of both transverse displacement, in-plane stresses, transverse shear stresses, and transverse normal stress for various thickness ratios. The performances of the plate element have been tested, and the different theories (classical and refined) within the CUF framework have been compared. The following conclusions can be drawn:

1. The plate element with the MITC technique is locking free, for all the ESL considered cases and for all the considered displacement theories. The results converge to the reference solution by increasing the order of expansion of the displacements in the thickness direction, regardless of the employed function type.

2. The zig-zag term is fundamental for the description of the transverse shear stress independently of the thickness ratio a/h.

3. The combination of the linear contribution with the trigonometric and exponential series is very important for the description of the displacement and stresses field. The linear contribution leads to the reduction of the trigonometric and exponential terms required to reach the reference solution.

4. The cosine series are more accurate with thin plate, $a/h = 100$. For thicker plates the cosine contribution is important for the description of transverse normal stress.

5. The sine series are effective for thicker plates. For thin plates the sine series can reach good results except for the transverse normal stress.

6. The exponential series lead to good results for all cases, especially for thicker plates.

7. For sandwich plates with weak core more accurate models are required. Using zig-zag models it is possible to take into account the discontinuous behaviour of the sandwich layered structures.

References

[1] W T Koiter. On the foundations of the linear theory of thin elastic shell. *Proc. Kon. Nederl. Akad. Wetensch.*, 73:169–195, 1970.

[2] P G Ciarlet and L Gratie. Another approach to linear shell theory and a new proof of Korn's inequality on a surface. *C. R. Acad. Sci. Paris*, I,340:471–478, 2005.

[3] P M Naghdi. The theory of shells and plates. *Handbuch der Physic*, 4:425–640, 1972.

[4] J N Reddy. An evaluation of equivalent-single-layer and layerwise theories of composite laminates. *Composite Structures*, 25:21–35, 1993.

[5] T Kant, D R J Owen, and O C Zienkiewicz. Refined higher order Cˆ0 plate bending element. *Computer & Structures*, 15:177–183, 1982.

[6] T Kant and J R Kommineni. Large amplitude free vibration analysis of cross-ply composite and sandwich laminates with a refined theory and Cˆ0 finite elements. *Computer & Structures*, 50:123–134, 1989.

[7] J N Reddy. Mechanics of laminated composite plates and shells. *Theory and Analysis, CRC Press*, 1997.

[8] A N Palazotto and S T Dennis. Nonlinear analysis of shell structures. *AIAA Series*, 1992.

[9] R P Shimpi and Y M Ghugal. A new layerwise trigonometric shear deformation theory for two-layered cross-ply beams. *Composite Science and Technology*, 61(9):1271–1283, 2001.

[10] H Arya, R P Shimpi, and N K Naik. A zigzag model for laminated composite beams. *Composite Structures*, 56(1):21–24, 2002.

[11] A J M Ferreira, C M C Roque, and R M N Jorge. Analysis of composite plates by trigonometric shear deformation theory and multiquadrics. *Computers and Structures*, 83(27):2225–2237, 2005.

[12] C M C Roque, A J M Ferreira, and R M N Jorge. Modelling of composite and sandwich plates by a trigonometric layerwise deformation theory and radial basis functions. *Composite Part B: Engineering*, 36(8):559–572, 2005.

[13] P Vidal and O Polit. A family of sinus finite elements for the analysis of rectangular laminated beams. *Composite Structures*, 84(1):56–72, 2008.

[14] P Vidal and O Polit. A sine finite element using a zig-zag function for the analysis of laminated composite beams. *Composite Part B: Engineering*, 42(6):1671–1682, 2011.

[15] A J M Ferreira, E Carrera, M Cinefra, C M C Roque, and O Polit. Analysis of laminated shells by a sinusoidal shear deformation theory and radial basis functions collocation, accounting for through-the-thickness deformations. *Composite Part B: Engineering*, 42(5):1276–1284, 2011.

[16] L Dong, A S El-Gizawy, K A Juhany, and S N Atluri. A Simple Locking-Alleviated 3D 8-Node Mixed-Collocation C0 Finite Element with Over-Integration, for Functionally-Graded and Laminated Thick-Section Plates and Shells, with & without Z-Pins. *Computers, Materials & Continua*, 41(3):163–192, 2014.

[17] E Carrera. Theories and finite elements for multilayered, anisotropic, composite plates and shells. *Archives of Computational Methods in Engineering*, 9(2):87–140, 2002.

[18] E Carrera. Theories and finite elements for multilayered plates and shells: a unified compact formulation with numerical assessment and benchmarking. *Archives of Computational Methods in Engineering*, 10(3):215–296, 2003.

[19] E Carrera, M Filippi, and E Zappino. Laminated beam analysis by polynomial, trigonometric, exponential and zig-zag theories. *European Journal of Mechanics A/Solids*, 41:58–69, 2013.

[20] E Carrera, M Filippi, and E Zappino. Free vibration analysis of laminated beam by polynomial, trigonometric, exponential and zig-zag theories. *Journal of Composite Materials*, 48(19):2299–2316, 2014.

[21] E Carrera, M Cinefra, , M Petrolo, and E Zappino. Finite Element Analysis of Structures Through Unified Formulation. *John Wiley & Sons Ltd*, 2014.

[22] N C Huang. Membrane locking and assumed strain shell elements. *Computers and Structures*, 27(5):671–677, 1987.

[23] C Chinosi and L Della Croce. Mixed-interpolated elements for thin shell. *Communications in Numerical Methods in Engineering*, 14:1155–1170, 1998.

[24] K J Bathe, P S Lee, and J F Hiller. Towards improving the MITC9 shell element. *Computers and Structures*, 81:477–489, 2003.

[25] E Carrera. Multilayered shell theories accounting for layerwise mixed description, Part 1: governing equations. *AIAA Journal*, 37(9):1107–1116, 1999.

[26] E Carrera. Multilayered shell theories accounting for layerwise mixed description, Part 2: numerical evaluations. *AIAA Journal*, 37(9):1117–1124, 1999.

[27] E Carrera. An assessment of mixed and classical theories for the thermal stress analysis of orthotropic multilayered plates. *Journal of Thermal Stresses*, 23(9):797–831, 2000.

[28] S Brischetto and E Carrera. Thermal stress analysis by refined multilayered composite shell theories. *Journal of Thermal Stresses*, 32(1-2):165–186, 2009.

[29] M Cinefra, E Carrera, and S Valvano. Variable Kinematic Shell Elements for the Analysis of Electro-Mechanical Problems. *Mechanics of Advanced Materials and Structures*, 22(1-2):77–106, 2015.

[30] H Murakami. Laminated composite plate theory with improved in-plane responses. *Journal of Applied Mechanics*, 53:661–666, 1986.

[31] K J Bathe and E Dvorkin. A formulation of general shell elements - the use of mixed interpolation of tensorial components. *International Journal for Numerical Methods in Engineering*, 22:697–722, 1986.

[32] M L Bucalem and E Dvorkin. Higher-order MITC general shell elements. *International Journal for Numerical Methods in Engineering*, 36:3729–3754, 1993.

[33] M Cinefra and S Valvano. A variable kinematic doubly-curved MITC9 shell element for the analysis of laminated composites. *Mechanics of Advanced Materials and Structures, In Press.*

[34] T J R Hughes, M Cohen, and M Horaun. Reduced and selective integration techniques in the finite element methods. *Nuclear Engineering and Design*, 46:203–222, 1978.

[35] N J Pagano. Exact solutions for rectangular bidirectional composites and sandwich plate. *Journal of Composite Materials*, 4:20–34, 1970.

[36] W J Liou and C T Sun. A three-dimensional hybrid stress isoparametric element for the analysis of laminated composite plates. *Computers and Structures*, 25:241–249, 1985.

[37] K Moriya. Laminated plate and shell elements for finite element analysis of advanced fiber reinforced composite structures. *Transactions of the Japan Society of Mechanical Engineering (Series A)*, 52(478):1600–1607, 1986.

[38] J N Reddy. A simple higher-order theory for laminated composite plates. *Journal of Applied Mechanics*, 51:745–752, 1984.

[39] H J Jing and M L Liao. Partial hybrid stress element for the analysis of thick laminated composite plates. *International Journal for Numerical Methods in Engineering*, 28:2813–2827, 1989.

[40] E Carrera and L Demasi. Classical and advanced multilayered plate elements based upon PVD and RMVT. Part 2: Numerical Implementations. *International Journal for Numerical Methods in Engineering*, 55:253–291, 2002.

[41] J N Reddy and W C Chao. A comparison of closed-form and finite-element solutions of thick laminated anisotropic rectangular plates. *Nuclear Engineering Design*, 64:153–167, 1981.

[42] B N Pandia and T Kant. Flexural analysis of laminated composites using refined higher-order Cˆ0 plate bending elements. *Computer Methods in Applied Mechanics and Engineering*, 66:173–198, 1985.

[43] S Di and E Ramm. Hybrid stress formulation for higher-order theory of laminated shell analysis. *Computer Methods in Applied Mechanics and Engineering*, 109:359–376, 1993.

[44] F Auricchio and E Sacco. A mixed-enhanced finite element for the analysis of laminated composite plates. *International Journal for Numerical Methods in Engineering*, 44:1481–1504, 1999.

[45] K M Liew, B Han, and M Xiao. Differential quadrature method for thick symmetric cross-ply laminates with first-order shear flexibility. *International Journal of Solids and Structures*, 33:2647–2658, 1996.

[46] E Carrera and A Ciuffreda. A unified formulation to asses theories of multilayered plates for various bending problems. *Composite Structures*, 69:271–293, 2005.

Tables

Table 1: Expansion terms of the proposed theories.

	$cost$	z^N				$(-1)^k\zeta_k$	$\sin\left(N\frac{z\pi}{h}\right)$					$\cos\left(N\frac{z\pi}{h}\right)$				$e^{\left(N\frac{z}{h}\right)}$					
$N=$		1	2	3	4		1	2	3	4	5	1	2	3	4	1	2	3	4	5	6
$ET4$	√	√	√	√	√	.	.	.	.	.	.	.	.	.	.	.	.	.	.	.	.
$ES5$	√	.	.	.	.	.	√	√	√	√	√	.	.	.	.	.	.	.	.	.	.
$ET1S1$	√	√	.	.	.	.	√	.	.	.	.	.	.	.	.	.	.	.	.	.	.
$ET1C1$	√	√	.	.	.	.	.	.	.	.	.	√	.	.	.	.	.	.	.	.	.
$EExp3$	√	.	.	.	.	.	.	.	.	.	.	.	.	.	.	√	√	√	.	.	.
$ET1Exp2$	√	√	.	.	.	.	.	.	.	.	.	.	.	.	.	√	√	.	.	.	.
$EExp4$	√	.	.	.	.	.	.	.	.	.	.	.	.	.	.	√	√	√	√	.	.
$ET1Exp3$	√	√	.	.	.	.	.	.	.	.	.	.	.	.	.	√	√	√	.	.	.
$ES3C3$	√	.	.	.	.	.	√	√	√	.	.	√	√	√	.	.	.	.	.	.	.
$ES4C4$	√	.	.	.	.	.	√	√	√	√	.	√	√	√	√	.	.	.	.	.	.
$ET1S1C1$	√	√	.	.	.	.	√	.	.	.	.	√	.	.	.	.	.	.	.	.	.
$ET1S2C2$	√	√	.	.	.	.	√	√	.	.	.	√	√	.	.	.	.	.	.	.	.
$ET3Z$	√	√	√	√	.	√	.	.	.	.	.	.	.	.	.	.	.	.	.	.	.
$ES4Z$	√	.	.	.	.	√	√	√	√	√	.	.	.	.	.	.	.	.	.	.	.
$ES5Z$	√	.	.	.	.	√	√	√	√	√	√	.	.	.	.	.	.	.	.	.	.
$ET1S2Z$	√	√	.	.	.	√	√	√	.	.	.	.	.	.	.	.	.	.	.	.	.
$ET1S3Z$	√	√	.	.	.	√	√	√	√	.	.	.	.	.	.	.	.	.	.	.	.
$ET1C2Z$	√	√	.	.	.	√	.	.	.	.	.	√	√	.	.	.	.	.	.	.	.
$EExp5Z$	√	.	.	.	.	√	.	.	.	.	.	.	.	.	.	√	√	√	√	√	.
$EExp6Z$	√	.	.	.	.	√	.	.	.	.	.	.	.	.	.	√	√	√	√	√	√
$ET1Exp4Z$	√	√	.	.	.	√	.	.	.	.	.	.	.	.	.	√	√	√	√	.	.
$ET1Exp5Z$	√	√	.	.	.	√	.	.	.	.	.	.	.	.	.	√	√	√	√	√	.
$ES4C4Z$	√	.	.	.	.	√	√	√	√	√	.	√	√	√	√	.	.	.	.	.	.
$ET1S3C3Z$	√	√	.	.	.	√	√	√	√	.	.	√	√	√	.	.	.	.	.	.	.

Table 2: Convergence study. Plate with lamination $[0°/90°/0°]$ and with thickness ratio $a/h = 100$.

	Mesh	4×4	6×6	8×8	10×10	$ET4_a$	$LW4$	$3D\ Exact\ Elasticity$[35]
$ET4$	w	0.4344	0.4343	0.4342	0.4342	0.4342	0.4347	-
	σ_{xz}	0.295	0.287	0.284	0.282	0.281	0.398	0.395
$ET1S1$	w	0.4294	0.4292	0.4292	0.4292			
	σ_{xz}	0.308	0.300	0.297	0.295			
$ET1Exp3$	w	0.4345	0.4343	0.4343	0.4343			
	σ_{xz}	0.315	0.307	0.304	0.302			
$ET3Z$	w	0.420	0.4347	0.4347	0.4347			
	σ_{xz}	0.4349	0.409	0.405	0.403			
$ET1C2Z$	w	0.4347	0.4346	0.4345	0.4345			
	σ_{xz}	0.414	0.403	0.399	0.397			

Table 3: Locking study. Plate with lamination $[0°/90°/0°]$ and with thickness ratio $a/h = 100$. All the cases are computed with a mesh of 10×10 elements.

		Reduced	*Selective*	$MITC9$	$ET4_a$	$LW4$	$3D\ Exact\ Elasticity$[35]
$ET4$	w	0.4342	0.4334	0.4342	0.4342	0.4347	-
	σ_{xz}	0.501	0.510	0.282	0.281	0.398	0.395
$ET1S1$	w	0.4292	0.4284	0.4292			
	σ_{xz}	0.511	0.526	0.295			
$ET1Exp3$	w	0.4343	0.4335	0.4343			
	σ_{xz}	0.521	0.538	0.302			
$ET3Z$	w	0.4347	0.4339	0.4347			
	σ_{xz}	0.621	0.673	0.403			
$ET1C2Z$	w	0.4345	0.4337	0.4345			
	σ_{xz}	0.614	0.675	0.397			

Table 4: Plate with lamination $[0°/90°/0°]$. Transverse displacement $\hat{w} = \hat{w}(a/2, b/2, +h/2)$, in-plane principal stress $\hat{\sigma}_{xx} = \hat{\sigma}_{xx}(a/2, b/2, \pm h/2)$, transverse shear stress $\hat{\sigma}_{xz} = \hat{\sigma}_{xz}(a, b/2, 0)$ and $\hat{\sigma}_{yz} = \hat{\sigma}_{yz}(a/2, b, 0)$.

	$a/h = 4$					$a/h = 100$					$DOFs$
	$\hat{w}$	$\hat{\sigma}_{xx}$		$\hat{\sigma}_{xz}$	$\hat{\sigma}_{yz}$	$\hat{w}$	$\hat{\sigma}_{xx}$		$\hat{\sigma}_{xz}$	$\hat{\sigma}_{yz}$	
		top	*bottom*				*top*	*bottom*			
$3D\ Exact\ Elasticity$[35]	-	0.801	-0.755	0.256	0.2172	-	0.539	-0.539	0.395	0.0828	
$LW4$	2.1216	0.807	-0.761	0.258	0.2197	0.4347	0.544	-0.544	0.398	0.0836	17199
$ET4_a$	2.0083	0.786	-0.740	0.205	0.1830	0.4342	0.539	-0.539	0.281	0.0734	
$ET4$	2.0082	0.793	-0.746	0.207	0.1845	0.4342	0.543	-0.543	0.283	0.0742	6615
$ES5$	2.0765	0.774	-0.779	0.293	0.2110	0.4294	0.541	-0.541	0.413	0.0451	7938
$ET1S1$	2.0089	0.772	-0.776	0.214	0.1857	0.4292	0.541	-0.541	0.295	0.0771	3969
$ET1C1$	1.6497	0.470	-0.426	0.122	0.1257	0.4332	0.543	-0.543	0.144	0.0605	3969
$EExp3$	1.9105	0.777	-0.604	0.177	0.1657	0.3945	0.497	-0.495	-0.303	-0.547	5292
$ET1Exp2$	1.9794	0.801	-0.696	0.198	0.1801	0.4341	0.544	-0.544	0.265	0.0731	5292
$EExp4$	2.0266	0.785	-0.747	0.223	0.1860	0.4323	0.541	-0.541	0.414	0.1664	6615
$ET1Exp3$	2.0199	0.785	-0.757	0.215	0.1850	0.4343	0.544	-0.544	0.302	0.0743	6615
$ES3C3$	2.0416	0.777	-0.732	0.245	0.1760	0.3781	0.474	-0.474	-0.435	-0.840	9261
$ES4C4$	2.0841	0.798	-0.752	0.287	0.1994	0.4324	0.541	-0.541	0.605	0.281	11907
$ET1S1C1$	2.0176	0.796	-0.752	0.213	0.1868	0.4342	0.544	-0.544	0.296	0.0747	5292
$ET1S2C2$	2.0448	0.788	-0.742	0.241	0.1821	0.4345	0.544	-0.544	0.376	0.0712	7938
$ET3Z$	2.1078	0.802	-0.756	0.259	0.1856	0.4347	0.544	-0.544	0.403	0.0709	6615
$ES4Z$	2.1116	0.783	-0.788	0.257	0.2209	0.4274	0.538	-0.538	0.586	0.2283	7938
$ES5Z$	2.1117	0.783	-0.788	0.257	0.2233	0.4295	0.541	-0.541	0.370	0.0591	9261
$ET1S2Z$	2.1084	0.782	-0.787	0.253	0.1975	0.4296	0.541	-0.541	0.401	0.0775	6615
$ET1S3Z$	2.1110	0.783	-0.788	0.255	0.2167	0.4296	0.541	-0.541	0.399	0.0843	7938
$ET1C2Z$	2.0461	0.709	-0.663	0.259	0.1741	0.4345	0.544	-0.544	0.397	0.0673	6615
$EExp5Z$	2.1134	0.805	-0.755	0.259	0.1899	0.4346	0.544	-0.544	0.426	0.1229	9261
$EExp6Z$	2.1180	0.805	-0.759	0.253	0.2032	0.4347	0.544	-0.544	0.403	0.0791	10584
$ET1Exp4Z$	2.1152	0.805	-0.758	0.257	0.1897	0.4347	0.544	-0.544	0.403	0.0725	9261
$ET1Exp5Z$	2.1186	0.806	-0.760	0.253	0.2023	0.4347	0.544	-0.544	0.402	0.0772	10584
$ES4C4Z$	2.1211	0.807	-0.761	0.257	0.2213	0.4324	0.541	-0.541	0.590	0.2283	13230
$ET1S3C3Z$	2.1206	0.807	-0.761	0.254	0.2172	0.4347	0.544	-0.544	0.401	0.0826	11907

Table 5: Plate with lamination $[0°/90°/0°]$ and thickness ratio $a/h = 10$. Transverse displacement $\hat{w} = \hat{w}(a/2, b/2, 0)$, in-plane principal stress $\hat{\sigma}_{xx} = \hat{\sigma}_{xx}(a/2, b/2, \pm h/2)$, transverse shear stress $\hat{\sigma}_{xz} = \hat{\sigma}_{xz}(a, b/2, 0)$ and $\hat{\sigma}_{yz} = \hat{\sigma}_{yz}(a/2, b, 0)$.

	$\hat{w}$	$\hat{\sigma}_{xx}$		$\hat{\sigma}_{xz}$	$\hat{\sigma}_{yz}$	$DOFs$
		top	*bottom*			
$3D\ Exact\ Elasticity$	0.7530	0.590	-0.590	0.357	0.1228	
$L\&S$ [36]	0.7546	0.580	-0.580	0.367	0.127	
$Moriya$ [37]	0.7512	0.5759	-0.5785	0.3993	0.1296	
$R-H$ [38]	0.7125	0.5684	-	0.1033	-	
$H\&L$ [39]	0.7531	0.5884	-0.5879	0.3627	0.1284	
$ET4(IS)$[40]	0.7268	0.5776	-0.5753	0.2948	0.1464	
$LW4$	0.7530	0.595	-0.595	0.3602	0.1238	17199
$ET4$	0.7151	0.588	-0.587	0.2639	0.1038	6615
$ES5$	0.7380	0.591	-0.592	0.4038	0.1194	7938
$ET1S1$	0.7142	0.588	-0.589	0.2746	0.1066	3969
$ET1C1$	0.6294	0.521	-0.521	0.1387	0.0759	3969
$EExp3$	0.6817	0.577	-0.550	0.2104	0.0852	5292
$ET1Exp2$	0.7066	0.588	-0.577	0.2484	0.1013	5292
$EExp4$	0.7254	0.589	-0.591	0.2993	0.1066	6615
$ET1Exp3$	0.7203	0.588	-0.591	0.2804	0.1046	6615
$ES3C3$	0.7310	0.586	-0.586	0.3434	0.0860	9261
$ES4C4$	0.7430	0.593	-0.592	0.4015	0.1149	11907
$ET1S1C1$	0.7192	0.591	-0.590	0.2754	0.1051	5292
$ET1S2C2$	0.7338	0.591	-0.590	0.3400	0.1030	7938
$ET3Z$	0.7528	0.596	-0.595	0.3646	0.1038	6615
$ES4Z$	0.7478	0.594	-0.594	0.3624	0.1273	7938
$ES5Z$	0.7478	0.594	-0.594	0.3583	0.1265	9261
$ET1S2Z$	0.7477	0.594	-0.594	0.3607	0.1122	6615
$ET1S3Z$	0.7478	0.594	-0.594	0.3598	0.1230	7938
$ET1C2Z$	0.7381	0.575	-0.575	0.3606	0.0973	6615
$EExp5Z$	0.7527	0.595	-0.594	0.3662	0.1072	9261
$EExp6Z$	0.7529	0.595	-0.594	0.3622	0.1142	10584
$ET1Exp4Z$	0.7528	0.595	-0.594	0.3642	0.1062	9261
$ET1Exp5Z$	0.7529	0.595	-0.594	0.3620	0.1136	10584
$ES4C4Z$	0.7530	0.595	-0.595	0.3636	0.1265	13230
$ET1S3C3Z$	0.7530	0.595	-0.595	0.3611	0.1222	11907

Table 6: Plate with lamination [0°/90°]. Transverse displacement $\hat{w} = \hat{w}(a/2, b/2, +h/2)$, in-plane principal stress $\hat{\sigma}_{xx} = \hat{\sigma}_{xx}(a/2, b/2, \pm h/2)$, transverse shear stress $\hat{\sigma}_{xz} = \hat{\sigma}_{xz}(a, b/2, 0)$ and $\hat{\sigma}_{yz} = \hat{\sigma}_{yz}(a/2, b, 0)$.

	$a/h = 4$					$a/h = 100$				
	$\hat{w}$	$\hat{\sigma}_{xx}$		$\hat{\sigma}_{xz}$	$\hat{\sigma}_{yz}$	$\hat{w}$	$\hat{\sigma}_{xx}$		$\hat{\sigma}_{xz}$	$\hat{\sigma}_{yz}$
		top	*bottom*				*top*	*bottom*		
$LW4$	2.1699	0.1106	-0.7960	0.1451	0.1215	1.0652	0.0851	-0.7217	0.1234	0.1234
$ET4_a$	2.1282	0.1093	-0.7708	0.2878	0.1091	1.0651	0.0842	-0.7157	0.2800	0.1120
$ET4$	2.1281	0.1100	-0.7770	0.2901	0.1100	1.0651	0.0849	-0.7215	0.2829	0.1132
$ES5$	2.1376	0.1031	-0.8334	0.2259	0.0831	1.0388	0.0905	-0.7124	0.1279	0.0511
$ET1S1$	2.0924	0.0990	-0.8109	0.3007	0.1149	1.0388	0.0905	-0.7124	0.3046	0.1218
$ET1C1$	2.0403	0.1025	-0.6585	0.2255	0.0871	1.0643	0.0867	-0.7231	0.2229	0.0891
$EExp3$	2.1144	0.1095	-0.7249	0.2846	0.1022	0.8801	0.0713	-0.5948	-0.8887	-0.9132
$ET1Exp2$	2.1204	0.1101	-0.7544	0.2965	0.1109	1.0650	0.0854	-0.7222	0.2924	0.1155
$EExp4$	2.1228	0.1080	-0.7546	0.3036	0.1012	1.0508	0.0832	-0.7125	0.9537	0.0877
$ET1Exp3$	2.1279	0.1090	-0.7683	0.3003	0.1041	1.0651	0.0848	-0.7218	0.2974	0.1070
$ES3C3$	2.1569	0.1101	-0.7917	0.2452	0.0902	0.8020	0.0640	-0.5429	-1.9729	-0.7892
$ES4C4$	2.1574	0.1104	-0.7911	0.2500	0.0917	1.0508	0.0838	-0.7119	0.7852	0.3141
$ET1S1C1$	2.1170	0.1109	-0.7657	0.2961	0.1142	1.0644	0.0867	-0.7233	0.2956	0.1182
$ET1S2C2$	2.1515	0.1119	-0.7897	0.2537	0.0940	1.0651	0.0852	-0.7219	0.2400	0.0960
$ET3Z$	2.1261	0.1095	-0.7674	0.2648	0.1293	1.0651	0.0851	-0.7217	0.2752	0.1351
$ES4Z$	2.1425	0.1087	-0.8103	0.2551	0.0824	1.0418	0.0872	-0.7109	0.9506	0.3623
$ES5Z$	2.1445	0.1090	-0.8112	0.2438	0.0777	1.0573	0.0885	-0.7214	0.1370	0.0352
$ET1S2Z$	2.1408	0.1088	-0.8102	0.2678	0.0879	1.0573	0.0885	-0.7214	0.2616	0.0850
$ET1S3Z$	2.1430	0.1089	-0.8106	0.2555	0.0827	1.0573	0.0885	-0.7214	0.2427	0.0775
$ET1C2Z$	2.0789	0.1042	-0.6984	0.1437	0.1207	1.0650	0.0853	-0.7219	0.1360	0.1233
$EExp5Z$	2.1595	0.1105	-0.7883	0.1770	0.1481	1.0642	0.0851	-0.7212	0.1654	0.2802
$EExp6Z$	2.1672	0.1098	-0.7960	0.1702	0.1352	1.0651	0.0850	-0.7217	0.0912	0.1205
$ET1Exp4Z$	2.1638	0.1107	-0.7940	0.1735	0.1443	1.0652	0.0851	-0.7217	0.1668	0.1499
$ET1Exp5Z$	2.1675	0.1099	-0.7963	0.1814	0.1358	1.0652	0.0851	-0.7217	0.1739	0.1399
$ES4C4Z$	2.1686	0.1103	-0.7957	0.1622	0.1386	1.0519	0.0840	-0.7127	0.1466	0.7019
$ET1S3C3Z$	2.1685	0.1105	-0.7956	0.1725	0.1352	1.0652	0.0851	-0.7218	0.1594	0.1382

Table 7: Plate of 4 layers $[0°/90°/90°/0°]$ with various thickness ratios a/h. Transverse displacement $\hat{w} = \hat{w}(a/2, b/2, 0)$.

a/h	4	10	20	100	$DOFs$
$3D\ Exact\ Elasticity$	1.937	0.737	0.513	0.435	
$R-H$ [38]	1.8937	0.7147	0.5060	0.4343	
$R-C$ [41]	1.7100	0.6628	0.4912	0.4337	
$P\&K$ [42]	1.8744	0.7185	-	0.4346	
$D\&R$ [43]	1.9530	0.7377	0.5122	0.4333	
$A\&S$ [44]	-	0.6693	-	-	
$LH\&X$ [45]	1.7095	0.6627	0.4912	0.4337	
$ET4(IS)$[40]	1.9506	0.7272	0.5112	0.4366	
$LW4$	1.9367	0.7370	0.5130	0.4346	22491
$ET4$	1.8708	0.7179	0.5073	0.4344	6615
$ES5$	1.9333	0.7267	0.5062	0.4294	7938
$ET1S1$	1.8995	0.7167	0.5032	0.4293	3969
$ET1C1$	1.4894	0.6244	0.4811	0.4332	3969
$EExp3$	1.7668	0.6844	0.4919	0.3953	5292
$ET1Exp2$	1.8435	0.7098	0.5050	0.4343	5292
$EExp4$	1.8905	0.7252	0.5095	0.4324	6615
$ET1Exp3$	1.8826	0.7218	0.5085	0.4344	6615
$ES3C3$	1.8956	0.7258	0.5074	0.3825	9261
$ES4C4$	1.9013	0.7273	0.5097	0.4318	11907
$ET1S1C1$	1.8818	0.7210	0.5082	0.4343	5292
$ET1S2C2$	1.8977	0.7271	0.5101	0.4345	7938
$ET3Z$	1.8715	0.7179	0.5073	0.4344	6615
$ES4Z$	1.9207	0.7235	0.5055	0.4277	7938
$ES5Z$	1.9336	0.7273	0.5070	0.4303	9261
$ET1S2Z$	1.9171	0.7233	0.5058	0.4303	6615
$ET1S3Z$	1.9214	0.7237	0.5059	0.4303	7938
$ET1C2Z$	1.4912	0.6244	0.4811	0.4332	6615
$EExp5Z$	1.8908	0.7254	0.5097	0.4344	9261
$EExp6Z$	1.9013	0.7275	0.5102	0.4345	10584
$ET1Exp4Z$	1.8912	0.7257	0.5097	0.4345	9261
$ET1Exp5Z$	1.9004	0.7274	0.5102	0.4345	10584
$ES4C4Z$	1.9014	0.7273	0.5097	0.4318	13230
$ET1S3C3Z$	1.9022	0.7275	0.5102	0.4345	11907

Table 8: Sandwich rectangular plate. Transverse displacement $w = w(a/2, b/2, \pm h/2)$, in-plane principal stresses $\sigma_{xx} = \sigma_{xx}(a/2, b/2)$ and $\sigma_{yy} = \sigma_{yy}(a/2, b/2)$.

	w		σ_{xx}				σ_{yy}			
	top	*bottom*	Top Skin		Bottom Skin		Top Skin		Bottom Skin	
			top	*bottom*	*top*	*bottom*	*top*	*bottom*	*top*	*bottom*
$LW4_a$[46]	-9.142	-8.968	-112.4	-48.435	-133.21	166.27	-52.824	-23.320	-54.327	69.915
$LW4$	-9.140	-8.968	-110.7	-51.073	-132.85	166.10	-50.519	-25.617	-53.664	69.254
$ET1_a$[46]	-0.1022	-0.1020	-89.63	-88.715	15.508	20.008	-51.453	-50.932	8.4375	11.041
$ET4$	-0.138	-0.137	-97.17	-101.32	7.580	27.82	-77.579	-85.692	10.330	42.724
$ES5$	-7.305	-7.286	-112.7	-56.801	-105.96	158.63	-66.121	-38.325	-42.071	81.605
$ET1S1$	-1.731	-1.638	-85.10	-85.295	-47.978	84.448	-35.870	-42.617	-43.629	58.979
$ET1C1$	-0.127	-0.129	-88.45	-87.420	14.642	20.492	-41.521	-40.932	6.314	9.564
$EExp3$	-4.371	-4.323	-92.47	-78.557	-76.505	113.58	-39.169	-41.849	-44.857	62.113
$ET1Exp2$	-2.765	-2.730	-90.87	-79.453	-45.443	82.566	-40.886	-39.775	-29.510	46.796
$EExp4$	-4.497	-4.434	-64.32	-104.42	-63.669	99.959	-11.174	-68.260	-30.944	47.640
$ET1Exp3$	-4.835	-4.756	-68.21	-98.110	-64.585	98.892	-15.117	-63.323	-28.370	43.578
$ES3C3$	-7.167	-7.043	-86.88	-82.210	-100.75	132.40	-28.679	-51.200	-41.649	54.757
$ES4C4$	-7.725	-7.584	-100.2	-64.880	-108.01	143.89	-42.273	-36.314	-43.099	60.993
$ET1S1C1$	-1.873	-1.859	-92.42	-80.000	-24.335	61.361	-43.735	-38.237	-16.651	34.028
$ET1S2C2$	-6.630	-6.513	-87.24	-78.839	-90.690	124.87	-30.876	-47.612	-36.754	52.577
$ET3Z$	-6.454	-6.358	-118.9	-62.869	-113.26	166.26	-62.580	-31.329	-60.878	94.730
$ES4Z$	-7.362	-7.184	-123.1	-42.628	-114.88	126.33	-65.387	-12.490	-54.109	47.247
$ES5Z$	-7.482	-7.303	-119.7	-45.595	-110.17	135.74	-61.693	-15.638	-48.151	55.481
$ET1S2Z$	-6.334	-6.166	-115.7	-51.880	-92.06	116.54	-59.280	-18.998	-41.748	47.515
$ET1S3Z$	-7.142	-6.968	-124.3	-42.770	-113.80	119.94	-66.762	-11.918	-55.304	42.962
$ET1C2Z$	-7.650	-7.516	-105.2	-54.839	-109.73	143.35	-48.303	-27.188	-45.287	60.373
$EExp5Z$	-7.606	-7.473	-108.1	-52.184	-108.58	142.57	-51.282	-24.240	-44.719	60.114
$EExp6Z$	-8.278	-8.126	-107.1	-52.842	-119.37	150.98	-48.835	-26.058	-48.859	62.350
$ET1Exp4Z$	-7.805	-7.665	-107.7	-52.359	-111.53	144.39	-50.512	-24.802	-45.700	60.124
$ET1Exp5Z$	-8.379	-8.225	-107.7	-52.612	-121.51	152.06	-49.329	-25.945	-50.000	62.425
$ES4C4Z$	-8.561	-8.403	-107.9	-52.185	-123.22	156.43	-49.162	-25.942	-49.863	65.144
$ET1S3C3Z$	-8.508	-8.351	-108.7	-51.973	-121.82	156.16	-49.995	-25.507	-49.019	65.342

Figures

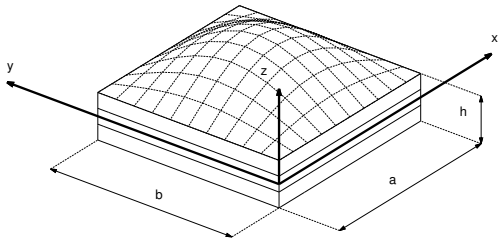

Figure 1: Reference system of the plate with a bi-sinusoidal loading.

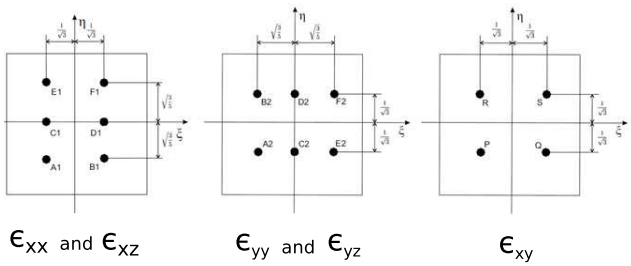

Figure 2: Tying points for the MITC9 plate finite element.

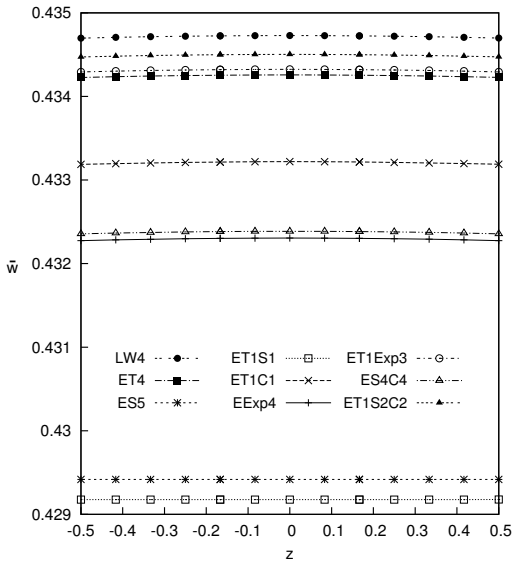

Figure 3: Transverse displacement $\boldsymbol{w}$ along the thickness, with thickness ratio $(a/h) = 100$.

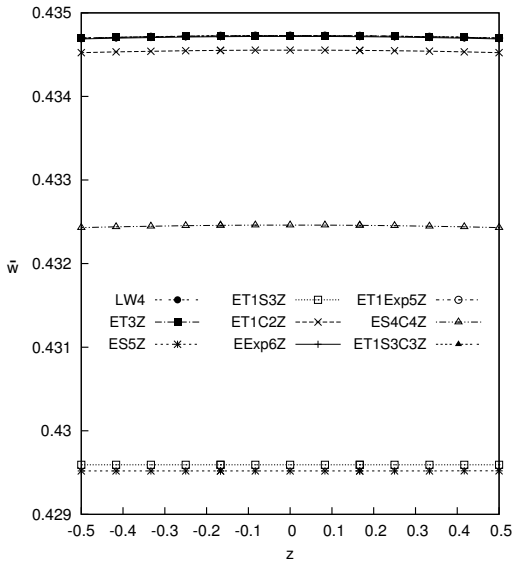

Figure 4: Transverse displacement $\boldsymbol{w}$ along the thickness, with thickness ratio $(a/h) = 100$.

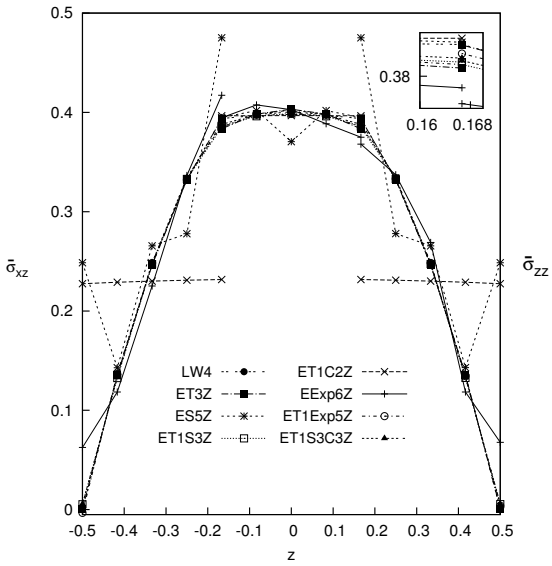

Figure 5: Transverse shear stress $\boldsymbol{\sigma}_{xz}$ along the thickness, with thickness ratio $(\,a\,/\,h\,) = 100$.

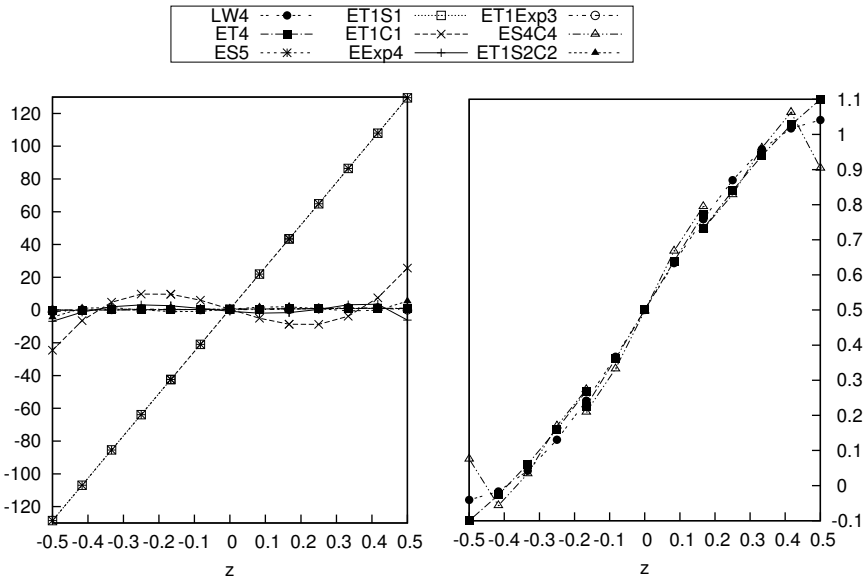

Figure 6: Transverse normal stress $\boldsymbol{\sigma}_{zz}$ along the thickness, with thickness ratio $(\,a\,/\,h\,) = 100$.

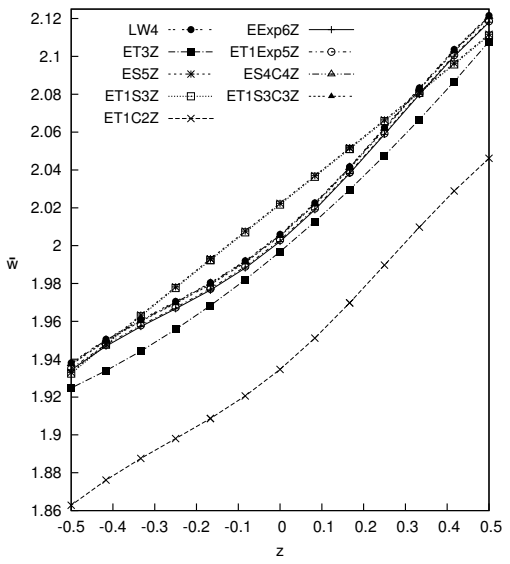

Figure 7: Transverse displacement $\boldsymbol{w}$ along the thickness, with thickness ratio $(\,a\,/\,h\,) = 4$.

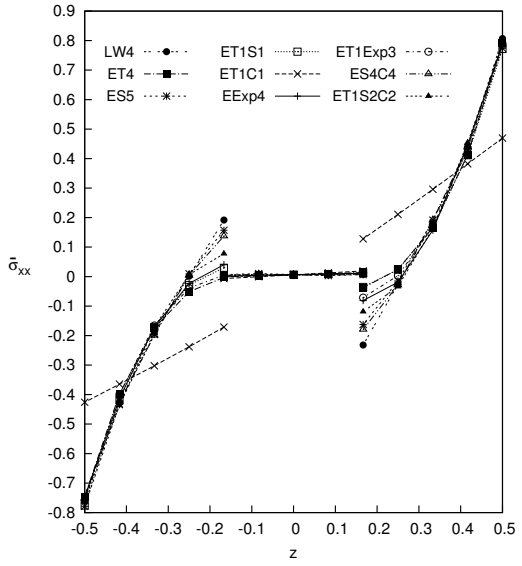

Figure 8: In-plane stress $\boldsymbol{\sigma}_{xx}$ along the thickness, with thickness ratio $(\,a\,/\,h\,) = 4$.

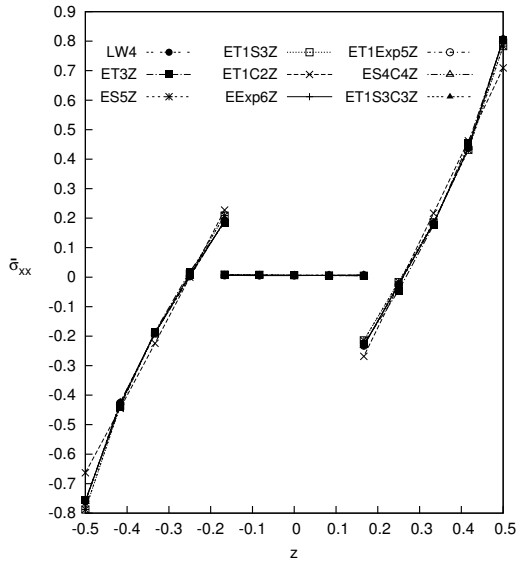

Figure 9: In-plane stress $\boldsymbol{\sigma}_{xx}$ along the thickness, with thickness ratio $(a/h) = 4$.

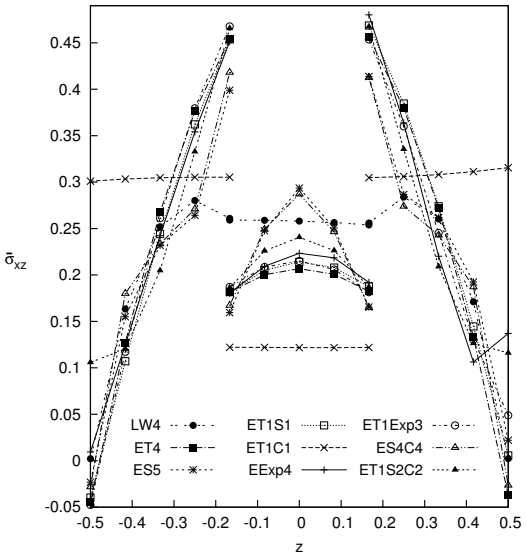

Figure 10: Transverse shear stress $\boldsymbol{\sigma}_{xz}$ along the thickness, with thickness ratio $(a/h) = 4$.

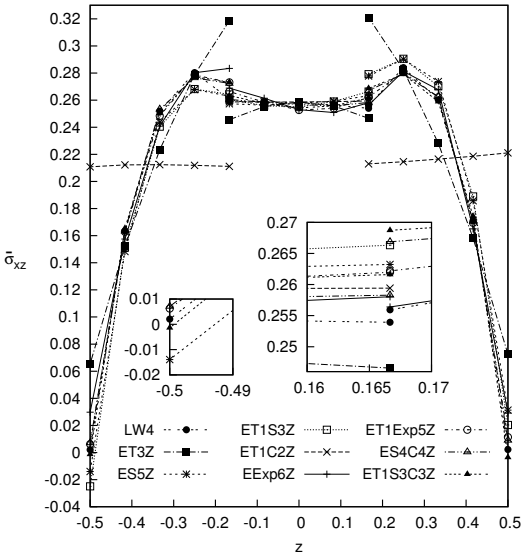

Figure 11: Transverse shear stress $\boldsymbol{\sigma}_{xz}$ along the thickness, with thickness ratio $(a/h) = 4$.

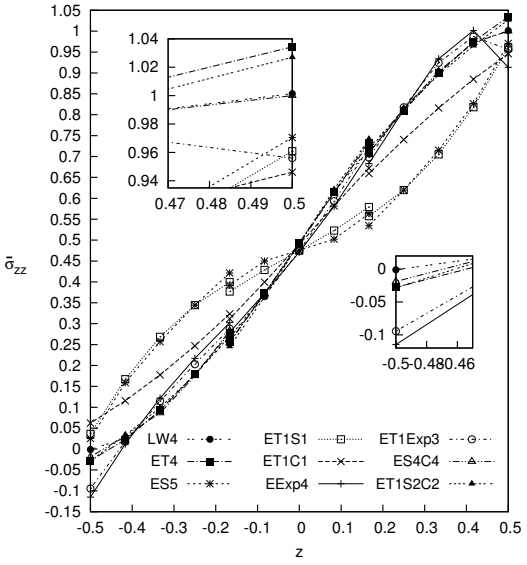

Figure 12: Transverse normal stress $\boldsymbol{\sigma}_{zz}$ along the thickness, with thickness ratio $(a/h) = 4$.

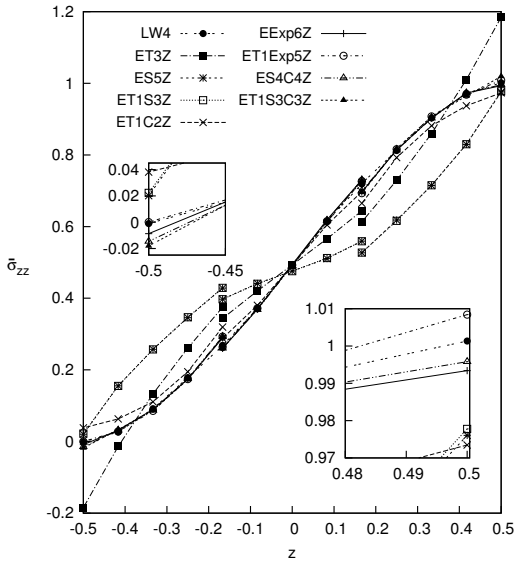

Figure 13: Transverse normal stress $\boldsymbol{\sigma}_{zz}$ along the thickness, with thickness ratio $(\,a\,/\,h\,) = 4$.

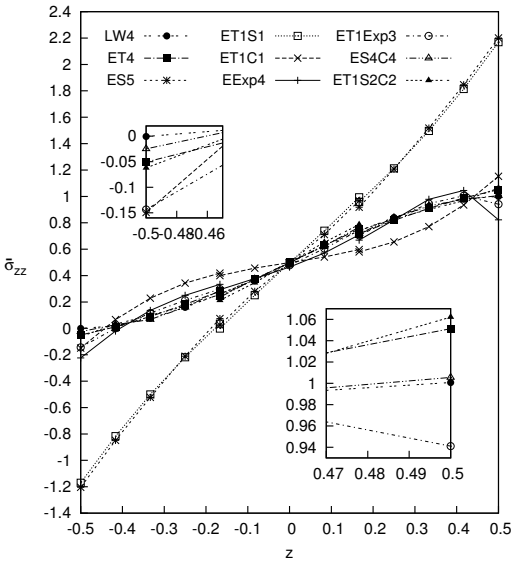

Figure 14: Transverse normal stress $\boldsymbol{\sigma}_{zz}$ along the thickness, with thickness ratio $(\,a\,/\,h\,) = 10$.